# X-Rays and Materials

Edited by
Philippe Goudeau
René Guinebretière

ISTE
WILEY

# Table of Contents

# X-Rays and Materials

Edited by
Philippe Goudeau
René Guinebretière

iSTE WILEY

First published 2012 in Great Britain and the United States by ISTE Ltd and John Wiley & Sons, Inc.



ISTE Ltd
27-37 St
London SW19
4EU
UK
www.iste.co.uk

John Wiley & Sons, Inc.
George's Road 111 River
Street
Hoboken, NJ 07030
USA
www.wiley.com



---

Library of Congress Cataloging-in-Publication Data

X-rays and materials / edited by Philippe Goudeau, René Guinebretière.

p. cm.

Includes bibliographical references and index.

ISBN 978-1-84821-342-5 (hardback)

1. Materials--Analysis. 2. X-ray microanalysis. 3. X-rays--Diffraction. 4. X-ray spectroscopy. I.

Goudeau, Philippe. II. Guinebretière, René.

TA417.25.X758 2012

620.1'1272--dc23

---

British Library Cataloguing-in-Publication Data
A CIP record for this book is available from the British Library
ISBN: 978-1-84821-342-5

# Preface [1]

This book presents reviews of various aspects of radiation/matter interactions, be these instrumental developments, the application of the study of the interaction of X-rays and materials to a particular scientific field, or specific methodological approaches. The overall aim of the book is to provide reference summaries for a range of specific subject areas within a pedagogical framework. Each chapter is written by an author who is well known within their field and who has delivered an invited lecture on their subject area as part of the “RX2009 – X-rays and Materials” colloquium that took place in December 2009 at Orsay.

For some years now, a new tool has been available in France for the exploration of the properties of materials through the use of X-rays. This is the SOLEIL synchrotron radiation source, which is now fully operational. It is able to respond to an ever-growing demand for “beam time”. It is also able to push the boundaries of certain areas of materials science. Our intention was that this book should be strongly focused on the use of synchrotron radiation.

This book consists of five chapters on the subject of X-ray diffraction, scattering and absorption.

Chapter 1 gives a detailed presentation of the capabilities and potential of beam lines dedicated to condensed matter studies at the SOLEIL synchrotron radiation source. After a general discussion of the source itself and the techniques involved, the authors of this chapter give a detailed discussion of the configurations that are available and the applications that have been developed around the “SAMBA”, “DIFFABS”, “CRISTAL” and “ODE” beam lines. Throughout this chapter, particular attention is paid to the discussion of how the different techniques can complement each other,

as well as the development of apparatus for measurement under thermal stress or high pressure.

When the objects interacting with the X-rays are nanometer-sized in addition to the diffraction signal that would be observed when they are crystallized, there is also a significant scattering contribution that appears around the center of the reciprocal lattice. This is referred to as “central X-ray scattering”, or more commonly as “small-angle scattering”. The pioneering work carried out by André Guinier has put the French scientific community in a strong position in this field. Bizarrely, few recent reviews pay much attention to this technique.

Chapter 2 focuses on the study of nanoparticles using small-angle X-ray scattering. It discusses in detail the formalism that can be used to interpret the scattering signal in terms of the size and shape of the particles that generate it. Extrapolation of the signal to the center of the reciprocal lattice space makes it possible to determine the volume of scattering material, and the author illustrates the potential of this technique with *in situ* monitoring of the seeding of gold nanoparticles.

Imperfections within the crystal lead to the appearance of localized “diffuse scattering”, which this time is not at the center of the reciprocal lattice but around the Bragg peaks. Since the discovery of carbon nanotubes around the start of the 1990s, their study has attracted a huge scientific community of chemists, biologists and condensed matter physicists. X-ray scattering is an ideal technique for performing quantitative measurements of the structural characteristics of carbon nanotubes: diameter, number of walls, lattice orientation, as well as examining the integration of fullerenes inside the tubes. Chapter 3 discusses the quantitative studies of this scattering signal used to analyze these characteristics in detail.

Chapter 4 discusses relaxor materials, which are ceramics with a particularly complex microstructure. These materials, with a paraelectric-ferroelectric transition temperature that is a function of the frequency of the applied electric field, consist of nanometer-sized regions with a different polarization to that of the matrix surrounding them. These are often associated with chemical inhomogeneities and local deformations of the crystal lattice. Here again, as in the previous chapter, diffuse scattering is observed around the Bragg peaks, and this provides information on these very specific microstructural characteristics.

The author of Chapter 4 is the head of a laboratory that has been heavily involved in this field for more than 20 years. He presents an in-depth discussion of this application area of X-ray diffraction and scattering. The reader will discover that the interpretation of this signal remains a highly controversial subject, but also that X-ray scattering is pivotal to the study of the nanometer-scale microstructure of these types of material.

The fabrication process for complex materials often includes thermal cycling, especially in metallurgy. The phase transitions that occur during these thermal treatments induce the appearance of specific microstructures that have a strong influence on the ultimate physical properties of the material. Chapter 5 discusses an approach enabling the *in situ* analysis of these phase transitions and their associated microstructural changes. Thus, the authors use a synchrotron to examine samples placed inside an oven, monitoring and quantifying the changes in the material using high-energy X-ray scattering. These measurements of the changes in lattice parameters and levels of transformed phases are performed with the help of a two-dimensional detector and, as a result, the acquisition times for the diagrams are in the order of a second, making it possible to observe the transformations occurring in real time.

[1] Preface written by René GUINEBRETIÈRE and Philippe GOUDEAU.

# Chapter 1

# Synchrotron Radiation: Instrumentation in Condensed Matter [1]

## 1.1. Introduction

Since the appearance of third-generation sources, the use of synchrotron radiation has seen a significant growth over a wide range of disciplines (biology, chemistry, physics, environmental science, earth science, cultural studies, etc.). The reasons behind this success are the qualities of the beams that can be obtained (flux, brilliance, stability, etc.) and the development of optics that are able to exploit these qualities to their full potential. To this we can add the possibility of setting up a sophisticated environment around the sample, enabling it to be monitored *in situ*.

In this chapter we intend to describe the various types of source available in a synchrotron radiation facility and define their brilliance. We will see how the optics can be adapted to particular types of experiments (generally X-ray absorption and diffraction) in order to best preserve this brilliance. We will illustrate this by describing some of the beam lines from the SOLEIL synchrotron. We will also give examples of the sample environments installed on these beam lines (we will limit ourselves to the field of condensed matter).

## 1.2. Light sources in the storage ring

Synchrotron radiation is generated by emissions from charged particles (electrons and positrons) undergoing centripetal acceleration. At first this emission was considered to be a parasitic element in particle collider rings constructed for particle physics experiments. Subsequently, however, it was realized that there were a range of applications for this radiation, and the designs were optimized with the intention of improving its characteristics.

The principle behind this involves packets of electrons circulating around what is known as a storage ring at a speed close to the speed of light. The storage ring consists of a succession of curved and straight sections. The various types of light source are installed in these two types of sections.

### 1.2.1. *Bending magnets*

In the curved sections of the storage ring, electrons emit white radiation (in other words radiation consisting of a mixture of all possible energies) tangentially to their trajectory and in a narrow cone with a vertical opening angle of ($\theta_{rms} = 1/\gamma$), which is manifest in the time domain as a succession of sharp intensity peaks. In energy space this corresponds to continuous emission, which leads to the term “white beam”. The emission spectrum depends on the energy of the machine, the number of electrons (machine current) and the magnetic field applied in the bending magnets. The emission spectrum in one of the SOLEIL bending magnets is shown in Figure 1.1.

The value of $\gamma$ depends on the machine energy; it represents is the Lorentz factor, given by:

[1.1] $$\gamma = \frac{E}{mC^2}$$

For SOLEIL [FIL 08], the energy of the electrons is $E$=2.75 GeV, giving $\gamma$= 5282 and $\theta_{rms}$ =0.186 mrad. The critical energy ($Ec$) corresponds to the division of the curve into two

parts of equal power ($P_0/2$). The higher the critical energy; the larger the number of high-energy photons that are available. The critical energy depends on the magnetic field of the bending magnets and the energy of the machine:

[1.2] $Ec\,(keV) = 0.665\,B(T)\,E^2\,(GeV)$

For the bending magnets of the beam lines discussed in this chapter, the critical energy is $Ec$ = 8.6 keV.

**Figure 1.1.** *Universal emission curve for a bending magnet*

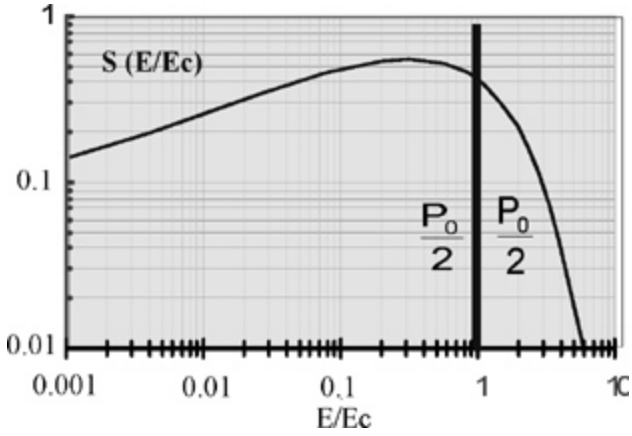


## 1.2.2. *Insertion devices*

It is also possible to create photon sources in the straight sections of the ring by introducing a succession of magnetic fields with opposing polarities. These are the insertion devices that cause the electrons to deviate from their course. This causes them to oscillate about the axis of the straight section. These insertion devices are characterized by the field strength ($B_0$) and the period ($\lambda_0$) of the magnetic field. The force of the insertion is defined by the parameter $K$:

[1.3] $K = 0.0934\,B_0(T)\,\lambda_0(mm)$

Two different variants exist depending on the value of $K$: undulators ($K < 1$) and wigglers ($K > 1$).

### 1.2.2.1. *Wigglers*

In the case of wigglers, the trajectory of the electrons oscillates with a large excursion from the axis of the straight section. The emission of light occurs in a horizontal layer of width $K/\gamma$, corresponding to the angular excursion of the electrons. In the vertical plane the radiation is emitted into an angle of $\pm 1/\gamma$, the same as for the bending magnets.

As viewed by an observer along the axis of the straight section, the emission is pulsed, with the time between successive emissions being the time taken for the electron to cross one period of the wiggler. This time-pulsed emission is associated with a broad-spectrum emission in energy terms. Thus, in the same way as with the bending magnets, we obtain a white beam. The different pulses of light add up in an incoherent manner, and the total flux is therefore proportional to the number of periods in the wiggler.

### 1.2.2.2. *Undulators*

In the case of undulators, $K$ is < 1. The trajectory of the electrons deviates only slightly from the axis of the straight section. At all points along its trajectory, the emission of light remains inside the relativistic emission cone $\alpha = 1/\gamma$ of the electron. For an observer on the axis of this synchrotron section, the emission is therefore continuous in time, giving an emission peaked at one particular energy. The light pulses emitted at each point along the trajectory add coherently, so that the overall flux (compared to that of an electron in a bending magnet) is multiplied by the square of the number of periods of the undulator. The magnetic field of the undulator is a function of the distance (or *gap*) between the magnetic poles of the undulator. The emission for a 9 mm gap in a U-20 type in-vacuum undulator, as used by SOLEIL, is shown in Figure 1.2 [BRI 06].

**Figure 1.2.** *Emission curve for a U-20 undulator with a gap of 9 mm by SOLEIL*

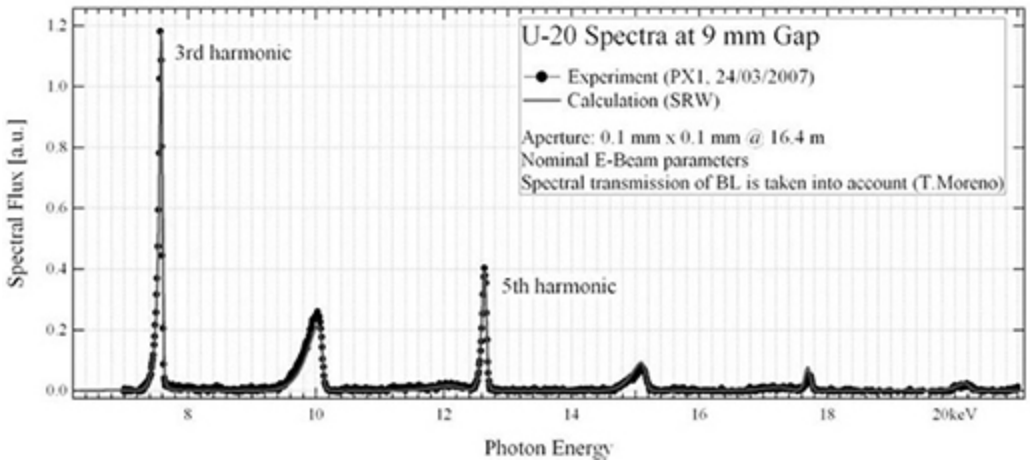


In order to cover the full range of energies, the value of the gap is altered, modifying the magnetic field applied and altering the energy of the harmonics.

## 1.3. Emittance and brilliance of a source

An important concept for a light source is its brilliance, which is defined by:

[1.4] $$B = \frac{N_{ph}}{dA\,d\Omega\,d\omega\,d\lambda/\lambda}$$

The brilliance is expressed as a number of photons per second, per mm$^2$ mrad$^2$ and for a bandwidth of 0.1%. Since we are some way from the diffraction limit, we can write:

[1.5] $$dA\,d\Omega = \varepsilon_x\,\varepsilon_z$$

where $\varepsilon_X$ and $\varepsilon_Z$ are the horizontal and vertical emittances of the electron beam. In other words, they are the product of the size of the source by its divergence in each plane. High source brilliance therefore results in a low emittance. The brilliance of a bending magnet is proportional to the number of electrons. The brilliance of a wiggler is proportional to the product of the number of electrons with the number of periods in the wiggler. The brilliance of an undulator is proportional to the number of electrons multiplied by the square of the number of periods. Undulator sources are

therefore by far the most brilliant sources. Conversely though, in an intermediate energy ring like SOLEIL (2.75 GeV), their critical energies are smaller than those obtained with a wiggler, where a more intense magnetic field is used (> 2*T*).

The brilliance is a constant of the source that can only be reduced by the optics used. It is a function of the number of photons per second, the size of the beam and its divergence. Any action to reduce the size (or divergence) of the beam can only increase the divergence (or size) or reduce the number of photons. The optic is chosen based on the experiment to be performed. Figure 1.3 gives a brief summary of this choice.

**Figure 1.3.** *Effects of optics depending on the experiment being performed (absorption, diffraction or monochromatization)*

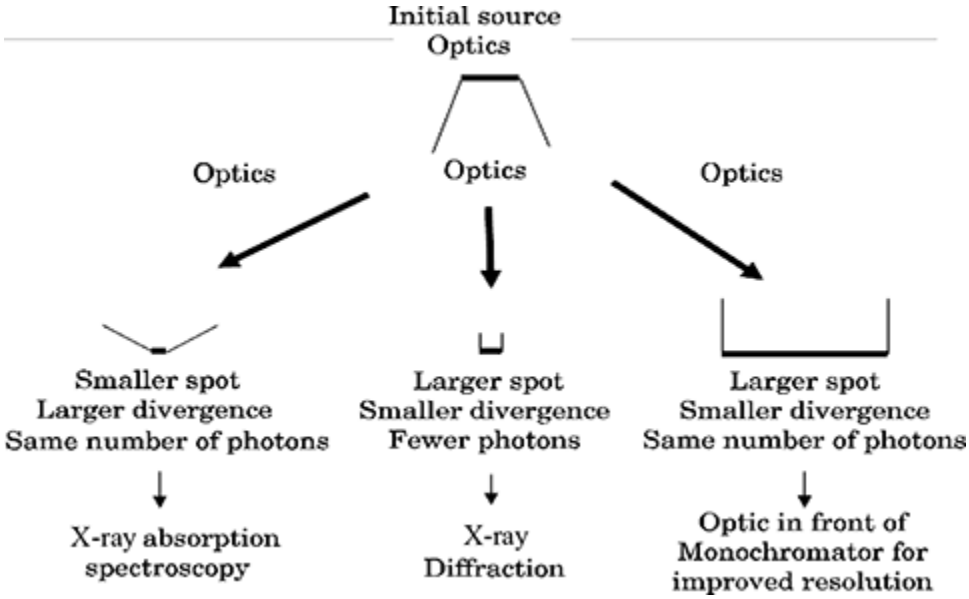


The optics on a beam line therefore depends on the nature of the source, the type of experiment to be performed, and the limitations associated with the sample environment (X-ray spot size, working distance of the optics, etc.). In the examples of beam lines given later on, the characteristics of the optics used will be described in association with the

experiments to be performed. It should be noted that the optics in a beam line are not necessarily fixed, and can be adapted to the specific needs of an experiment. It is possible to switch from a focused to an unfocused mode, or from a monochromatic mode to a white beam mode (in the latter case this possibility must be built into the light source from the start, since, for example, the radiological safety conditions are not the same in each case).

## 1.4. X-ray diffraction with synchrotron radiation

X-ray diffraction with synchrotron radiation can be studied using two different methods: angular dispersion of a monochromatic beam, and energy dispersion (which requires a white beam). As we will see later on, the two techniques can be coupled together.

### 1.4.1. *Angle-dispersive diffraction*

Angle-dispersive diffraction is identical to the diffraction seen in the laboratory with a classical X-ray source (tube or rotating anode). It is measured using a monochromatic beam, with detection being at varying angles. The advantages of a synchrotron are:

– the greatly improved brilliance of the source, resulting in a better final resolution and a larger number of photons in a smaller spot, which opens up the possibility of time-resolved work and/or microbeam work;

– the choice of photon wavelength, making it possible to avoid or exploit (anomalous diffraction) the absorption edges of the elements that make up the material being studied;

– the possibility of working at short wavelengths (< 0.3 Å), which reduces the angular domain in reciprocal space

(compatible with sample environments with limited apertures); and

– good accessibility around the sample, enabling the use of a complex sample environment (cryostat, high pressure cells, electrochemical cells, etc.).

These points will be expanded on and illustrated with application examples a little later on, when we describe the DIFFABS and CRISTAL beam lines.

For detection, increasing use is being made of two-dimensional detectors with fixed positions (imaging plate or large-scale CCD (charge coupled device)) or detectors mounted on a diffractometer arm (four or six circles), which can give faster and more efficient data acquisition. Point detectors and one-dimensional detectors are still used in certain applications (high-resolution X-ray diffraction and X-ray reflectometry, for example).

### 1.4.2. *Energy dispersive diffraction*

Energy dispersive diffraction is only used with synchrotron radiation because this results in an intense white beam, which is something that is not available as a laboratory source. The technique involves the acquisition, at one single angle, of the diffraction peaks obtained when the sample (in powder form) is exposed to the white beam. The energy of the diffracted peaks is determined using a solid-state detector (generally a Ge detector, as these are more sensitive at high energies). Their intensity is obtained using a multi-channel analyzer linked to the detector, which counts the number of events that occur at each energy peak. Bragg's law can then be applied, exchanging the standard roles of the diffraction angle, $\theta$, and the wavelength (or rather the energy) of the X-ray photons for a lattice spacing, $d$, expressed in Angstroms:

[1.6] $$d = \frac{6.199}{E(keV)\sin(\theta)}$$

This technique is widely used with second-generation synchrotrons, particularly in high-pressure experiments, but it has somewhat fallen out of favor due to the expense of monochromatic beam measurements on third-generation synchrotron sources, in view of the brilliance of undulator sources.

Figure 1.4 shows an example of a phase transition under pressure as monitored by energy dispersive diffraction [KUZ 05] (the spectra were obtained using the DCI wiggler source, LURE). The change in the diffraction spectrum can clearly be seen, starting at 8.4 GPa, with the transition being complete by 16.2 GPa.

**Figure 1.4.** *Evolution under pressure of the diffraction spectrum of $SrWO_4$ measured using energy dispersive diffraction*

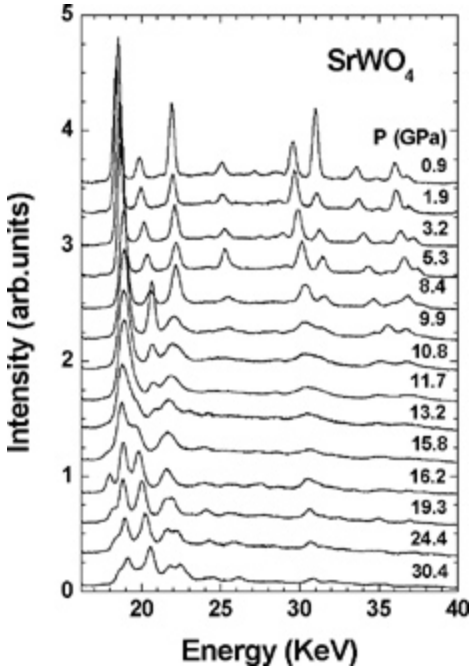


The geometry of energy dispersive diffraction (see Figure 1.5) makes it possible to choose the part of the sample to be studied, acting like a Soller slit. This is important for *in situ* measurements, since it makes it possible to strongly reduce the signal generated by the sample environment.

**Figure 1.5.** *Geometry for energy dispersive diffraction. The intersection of the incident beam and the beam that hits the detector defines the diffraction parallelogram*

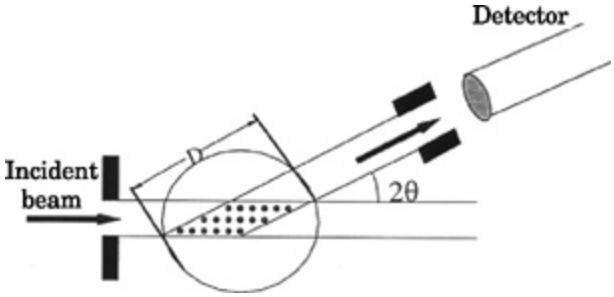


This technique has a number of advantages and disadvantages.

The advantages are:

– three-dimensional spatial resolution (use in imagery);

– no detector movement during acquisition; and

– rapid acquisition, due in part to the high flux (> 1,012 ph/s in 10 µm × 10 µm).

The disadvantages are:

– escape peaks caused by the detector (which are detectable by making use of the energy difference for $K_\alpha$ and $K_\beta$ in germanium);

– sample fluorescence (which is independent of the chosen angle, and known);

– point detection (a conical slit system can be used to recover the entire diffraction ring, but this requires a large-sized detector or a multidetector);

– energy-dependent absorption correction (which is proportional to the background); and

– detector resolution (which is 0.4% to 2%, depending on energy).

For certain applications it is possible to combine both techniques (angular dispersion and energy dispersion) by mounting the germanium detector on a theta arm [WAN 04] and recording the energy dispersion spectrum using a white

beam for each angular step. This results in a three-dimensional diagram giving the intensity as a function of angle and energy (see Figure 1.6).

**Figure 1.6.** *Angle-energy-intensity diagram obtained using the CAESAR technique [WAN 04]. The arrows show the directions of increasing angle and energy (proportional to the channel number). MCA — multi-channel analyzer*

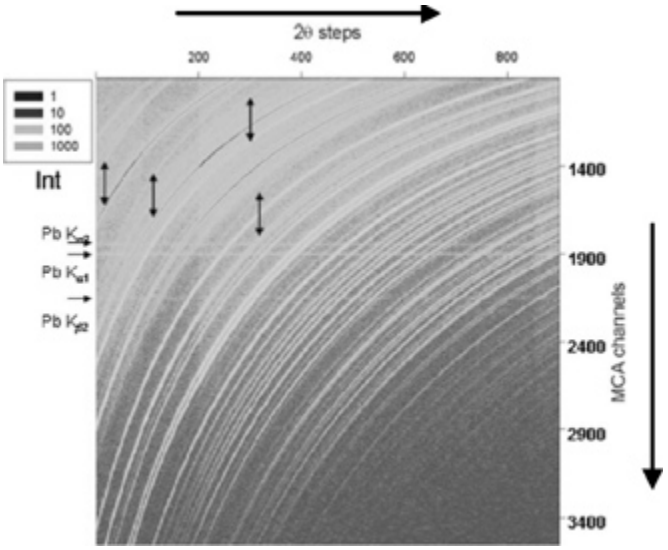


The diffraction diagram can be reconstructed either for fixed energy (see Figure 1.7) or for a fixed angle.

It is also possible to combine the data obtained for different energies by using Bragg's law to express them as a function of energy and angle: a point obtained at $E + \delta E$ and an angle $\theta$ can be written in terms of $E$ and $\theta + \delta\theta$ using the following equation:

[1.7] $$(E+\delta E)\sin(\theta) = E\sin(\theta+\delta\theta)$$

This makes it possible to increase the angular step of the acquisition while still retaining sufficient resolution in the diffraction spectrum (a variation from 50 eV to 50 keV corresponds to an angular displacement of 0.01°).

**Figure 1.7.** *Diffraction diagram extracted from the diagram shown in Figure 1.6 at an energy level of 74.956 keV [WAN 04]*